

Synthesis, Characterization, Photocatalytic and Photovoltaic Applications of a Novel Semiconductor CuPbO Nanomaterial

P. PONNAMBALAM¹, J. KAMALAKANNAN², R. JAYASEELAN³, M. AROKIA DOSS⁴ and G. SELVI^{1,5,*}

¹Research and Development Centre, Bharathiar University, Coimbatore-641046, India

²PG & Research Department of Chemistry, Srivinyaya College of Arts and Science, Ulundurpet-606213, India

³PG Department of Chemistry, Dr. R.K.S. College of Arts and Science, Kallakurichi-606213, India

⁴Department of Chemistry, St. Joseph University, Dimapur-797115, India

⁵Department of Chemistry, P.S.G.R. Krishnammal College for Women, Peelamedu, Coimbatore-641004, India

*Corresponding author: E-mail: selvi_gv@rediffmail.com

Received: 25 July 2021;

Accepted: 22 September 2021;

Published online: 16 December 2021;

AJC-20627

A new semiconductor CuPbO nanomaterial has been prepared where lead nitrate and copper nitrate were co-precipitated to form this compound. The high-resolution scanning electron microscopic studies revealed that CuPbO possesses a nanobundle flower-like structure. XRD confirmed the occurrence of Cu, Pb & O in the fabricated compound. The size of the nanomaterial is determined for being ~200 nm by high-resolution transmission electron microscopic analysis. The photoluminescence analysis showed the possible electron transfer and crevasses between Cu and PbO causes recombine of electron-hole pairs. The ultraviolet-visible diffuse reflectance spectral analysis showed that the nanomaterial has a low band gap energy. The material was found to be a good recyclable photocatalyst in the decomposition of diamond green B dye. As a photoelectrode, CuPbO proved its efficiency in dye-sensitized solar cell applications.

Keywords: Co-precipitation, Semiconductor oxide, Diamond green B dye, Photocatalysis, Dye-sensitized solar cell.

INTRODUCTION

The discharge of large quantity of coloured water from industries poses a threat to the environment. The existence of dyes in polluted water colouration, which might interfere with photosynthesis and hence have an impact on the aquatic ecology, UV-visible light is absorbed by the coloured molecules, reducing the amount of light available for photosynthesis. Photocatalytic degradation of organic dyes is gaining popularity as a viable possible treatment. Many fields of chemistry, physics and material science are interested in transition metal oxides with nanostructure. As a result, efforts are being undertaken to develop materials with absorption ranging into the visible range, giving for the use of majority of the solar spectrum. Lead(II) oxide nanoparticles can be synthesized by different methods [1-6]. A number of systems containing transition metal doped TiO₂ [7], nitrogen doped TiO₂ [8] have been reported for the photosensitization of dye pollutants [9,10].

Diamond green B dye has several industrial applications. It is used as a fungicide, ectoparasiticide and antiseptic in fish

farming industry. This is also used to dye leather, silk, paper and plastics [11]. This dye may be easily reduced to its leuco form, which is carcinogenic to humans [12]. For all these reasons, the development of innovative technologies of wastewater purification is essential [13-22].

EXPERIMENTAL

Lead nitrate, copper nitrate, hydrochloric acid, diamond green B dye (hexadecimal colour code #b9cca6, an anthocyanin dye emitted from real blueberry fruit extract), fluorine doped tin oxide (FTO)-plate, ruthenium dye (535-bisTBA, N719) solution and ethanol were obtained from Sigma Aldrich, USA and used as received. Throughout the studies, glasswares were cleansed with chromic acid and then carefully washed with distilled water.

Synthesis of CuPbO nanomaterial: Lead nitrate and copper nitrate hexahydrate were mixed in a 1:1 ratio in 100 mL deionized water and stirred vigorously at room temperature. Then solution was sonicated for 20 min. Also with

inclusion of ammonia solution, the pH of the solution was boosted to around 9. A precipitate was generated by mixing 5 drops conc. HNO_3 with 5 mL distilled water. The alkali phases were recovered by filtering the residue and washing with 10 mL ethanol. The residue was again collected and dried in an hot air oven at 100°C for 12 h. The powdered was then annealed for 3 h at 500°C .

Characterization: The surface morphology of CuPbO HR-SEM has been used to investigate using JEOL-JES-1600 instrument. At 25°C , EDX assessment trials were carried out on an FEI Quanta FEG 200 apparatus equipped with an EDX analyzer. A JEOL-JEM-2010 UHR apparatus was used to obtain a high-resolution transmission electron microscopy (HR-TEM) pictures with a lattice image resolution of 0.14 nm and an acceleration voltage of 200 kV. The X-ray diffraction using a Shimadzu-6000 (monochromatic $\text{CuK}\alpha$ radiation, $\lambda = 1.5406 \text{ \AA}$) apparatus was used to investigate the nanomaterial's crystalline characteristics. At room temperature, the XRD pattern was recorded in the 2θ range of 10° to 90° with 0.05° steps. At room temperature, the photoluminescence (PL) spectra of PbO and CuPbO were obtained using a Perkin-Elmer LS 55 fluorescence spectrometer. A Hitachi-U-2001 spectrophotometer was used to measure UV-Vis absorbance across a range of 800-

200 with a quartz cell with a 10 mm optical path length. On a Shimadzu UV-1650PC spectrophotometer the UV-vis DRS of PbO and CuPbO were measured. The photovoltaic parameters of the material were investigated by monitoring the photo current-voltage (I-V) curve under Ampere metres (A.M) 1.5 sun irradiation with a current density of 100 Mw/cm^2 .

RESULTS AND DISCUSSION

Evaluation of exterior microstructures

HR-SEM evaluation via EDX: The HR-SEM image of the CuPbO nanomaterial is shown in Fig. 1a. The material exhibited a uniform nanobundle flower like morphology with an abundance of grain boundaries. The observed pores indicate the possible catalytic sites for adsorption and photodegradation. The EDX spectrum was acquired to examine the nanocatalyst's appropriate quantity, which shows the presence of Cu, Pb and O (Fig. 1b).

HR-TEM: HR-TEM pictures revealed more about the structure of the CuPbO nanomaterial that has been developed. The images exhibit a typical intercrossed nanoribbon structure (Fig. 2a). The CuPbO nanomaterial has a dimension of around 200 nm. A picture profile based on particle size in a specified

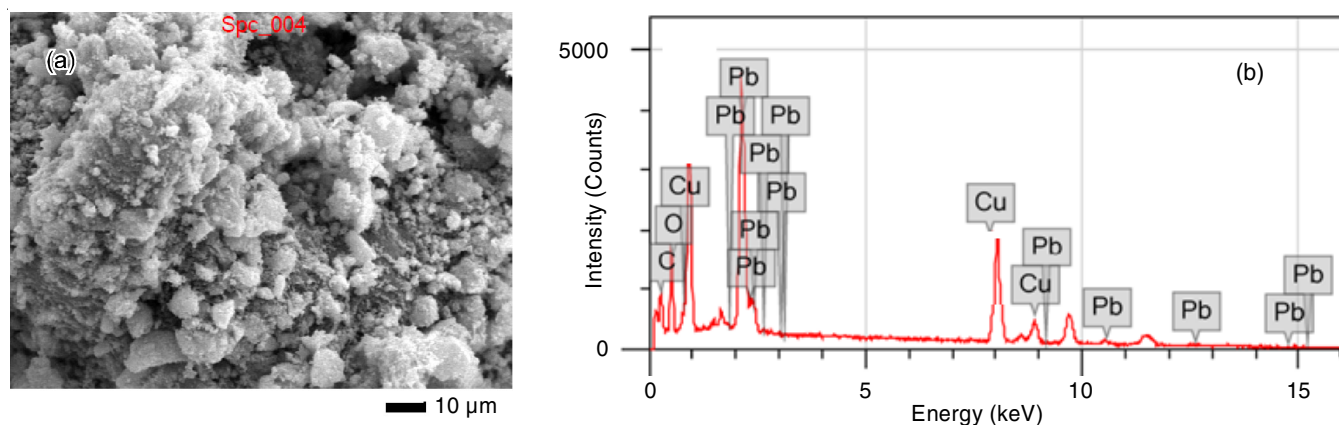


Fig. 1. (a) SEM image of CuPbO nanomaterial and (b) EDS analysis

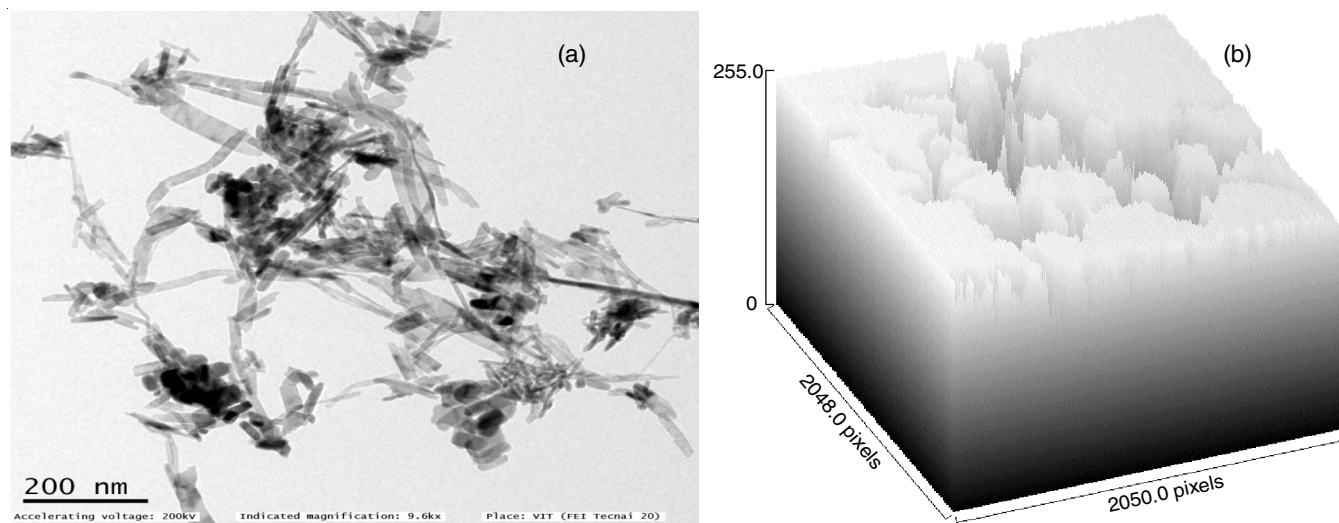


Fig. 2. (a) HR-TEM micrograph of CuPbO nanomaterial (b) Image profile from particle size in selected area highlighted

area marked in Fig. 2a is shown in Fig. 2b. The “Image J Viewer” software was used to calculate the image aspect distribution.

XRD analysis: The XRD pattern of CuPbO (Fig. 3) exhibited characterized peaks (2θ) at 29.1° , 30.4° , 32.5° , 37.7° , 49.4° , 50.9° , 53.3° , 56.2° and 63.7° corresponding to 111, 002, 200, 210, 022, 220, 222, 311 and 131, respectively. The XRD pattern is consistent with the structure of lead oxide (JCPDS Card No. 76-1796) with space group $Pca2_1$. The spiky peaks indicate the excellent crystalline nature of lead oxide nanomaterial and the broad peaks indicate that the particles are in superior agreement with the SEM images. $L = 0.89/\text{COS}$, the particle size computed using the Debye-Scherrer formula was found to be 24 nm.

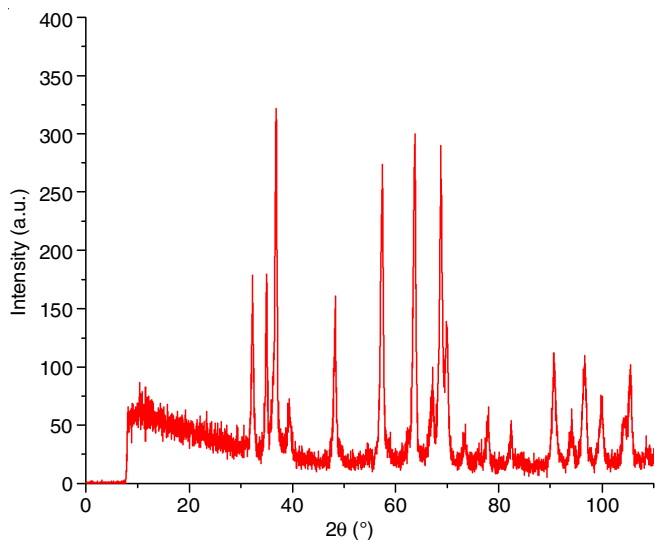


Fig. 3. XRD analysis of CuPbO nanomaterial

Photoluminescence (PL) studies: The coupling of electric charge causes spectroscopy to occur. As a result, charge carrier pairings and trapping may be studied using PL spectra. The PL emission of PbO and CuPbO in the 350-500 nm region is shown in Fig. 4a and 4b, respectively. The emissions peaks

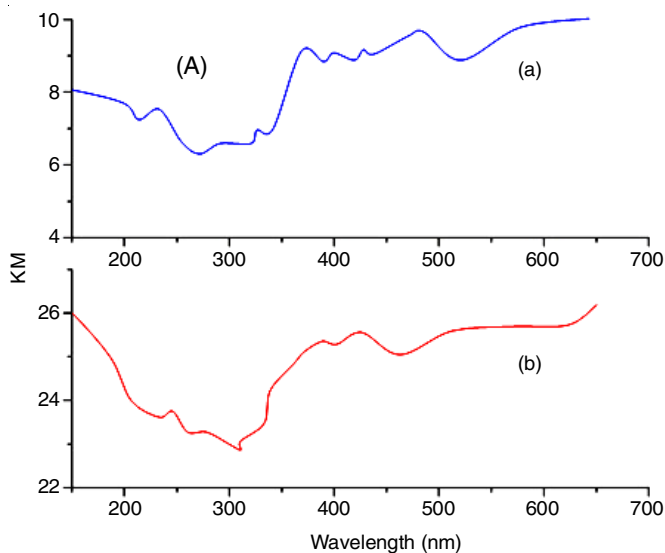


Fig. 5. UV-vis DRS-direct band gap of (a) PbO and (b) CuPbO nanomaterial

for the bare PbO nanoparticle are about 368, 403, 440 and 487 nm. CuPbO on the other hand, has a broad emission peak in the range of 350 to 500 nm, concentrated around 375 nm. The peak position indicates that it is caused by defect emission [23-25]. The large red-shifted peak is consistent with CuPbO's UV-vis-DRS. This is caused by the alteration of the band structure of PbO caused by Cu doping. When compared to PbO, CuPbO showed a considerable drop in PL intensity, indicating that CuPbO had a reduced photogenerated charge carrier recombination rate. Doping was discovered to reduce trap states on the material surface and inhibit the recombine of electrolyte ions in PbO. As a result the charge carrier separation improves and PbO's quantum efficiency improves.

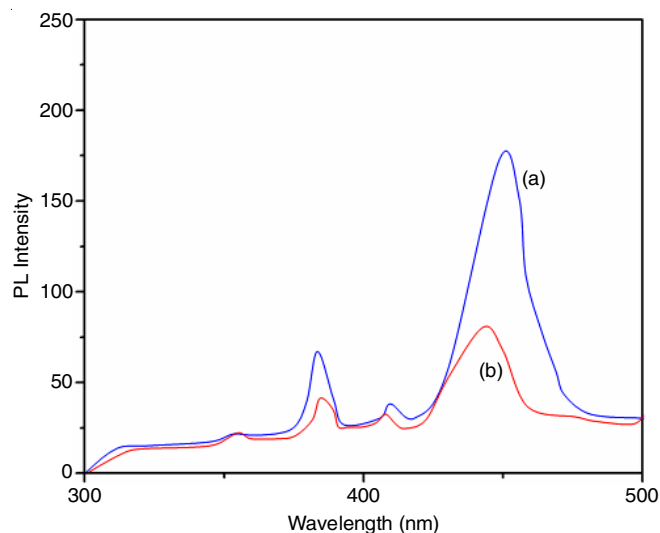


Fig. 4. PL spectra of (a) PbO and (b) CuPbO nanomaterial

UV-vis-DRS studies: Fig. 5a-b shows the UV-Vis-DRS spectra of generated PbO and CuPbO nanomaterial. The Tauc plots could be used to determine the band gaps of the synthesized nanomaterials. The band gap of the synthesized bulk CuPbO nanomaterial is determined by plotting $[F(R)hv]^2$ versus

the photon energy ($h\nu$). The width effect occurs for the blue shift in PbO nanoparticle. The PbO and CuPbO nanomaterials have suitable band energies of 2.8 and 2.5 eV, respectively. This study reveals that CuPbO has a lower band gap energy, suggesting that it could be used as a photocatalyst [26-29].

Photodegradation of diamond green B dye: With artificial UV-light irradiation, the photodegradation of diamond green B dye was studied in deionized water, distilled water and contaminated saltwater. At a concentration of 1×10^{-4} M, the aqueous solution of diamond green B dye was black in colour. After the photodegradation (45 min of irradiation time), the colour disappeared and the solution became colourless. The photodegradation investigations were performed out under different conditions, including those in which there was no energy. catalyst and in dark. The photodegradation profiles of the dye by PbO and CuPbO after 45 min of irradiation are shown in Fig. 6a-c. In deionized water, the efficiency was 12%, 5%, 95%, 56% and 45% without catalyst, under dark condition, with CuPbO catalyst and PbO catalyst, respectively. In distilled water, the efficiencies in the same order mentioned above were 9%, 6%, 79% and 43%. In contaminated seawater, the efficiency was 4% without the catalyst, 3% under dark condition, 42% when CuPbO was used as catalyst and 32% when PbO was used as catalyst. Comparison of the results shows that CuPbO photodegrades diamond green B dye to a greater extent in deionized water than in distilled or contaminated seawater.

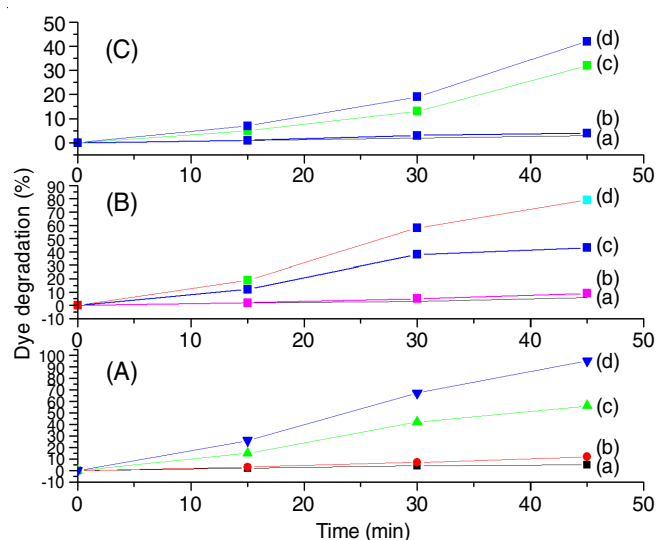


Fig. 6. Effect of degradation study of DG B dye under UV-light irradiation in (A) deionized water and (B) distilled and (C) sea water under the conditions of (a) dark (b) without catalyst (c) PbO catalyst and (d) CuPbO catalyst

Stability of photocatalyst: The system has better durability and reusability, which are extremely crucial by repeating diamond green B dye photocatalytic degradation studies four times, these features of PbO and CuPbO were studied. The photocatalysts were carefully rinsed with water after each cycle and a new solution of diamond green B dye was prepared before every photocatalytic run in the photoreactor under UV light and the results are shown in Fig. 7a-c. In deionized water (59 and 98%), distilled water (21 and 62%) and polluted sea

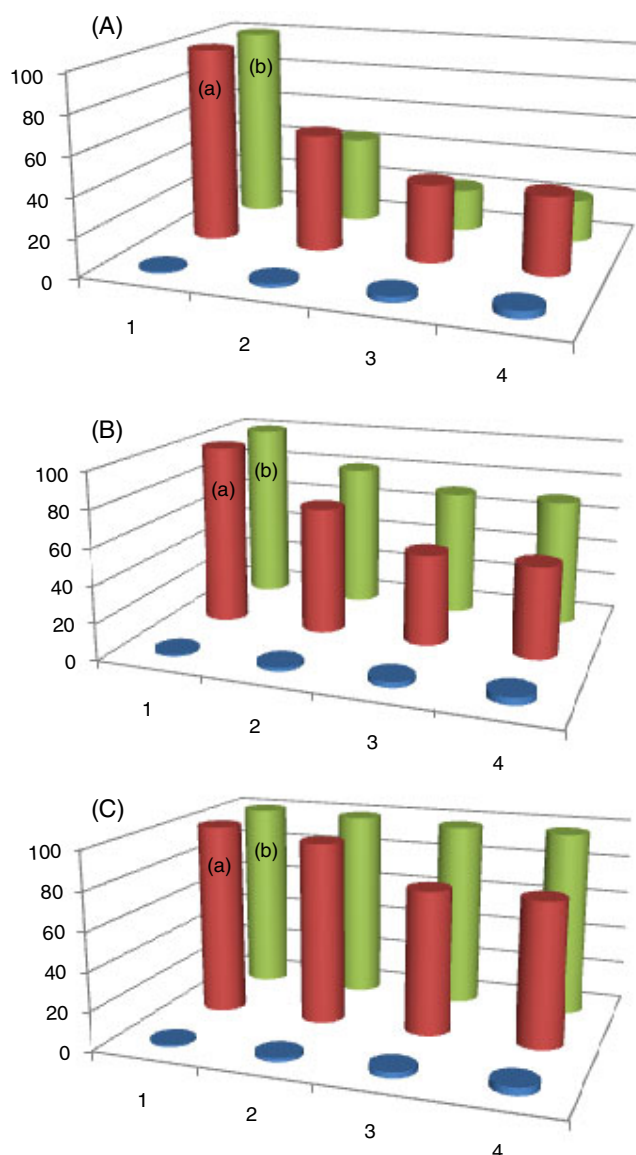
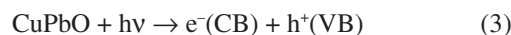


Fig. 7. Stability and reusability of the catalysts [(a) PbO and (b) CuPbO] in (A) deionized water and (B) distilled and (C) sea water under

water, total deterioration occurred in 45 min up to the 4th cycle (16 and 20%). The produced photocatalysts were successfully synthesized and reusable. In comparison to the entire breakdown of diamond green B dye, catalyst performance dropped after the fourth cycle consequently the response did not alter significantly, showing that the catalyst was stable. In fact, the CuPbO photocatalyst is harmless. As a result, CuPbO photocatalyst can be utilized to photodegrade impurities with good sensitivity and recyclability.

Photocatalytic mechanism: A possible mechanism to degrade diamond green B dye photocatalytically by CuPbO can be proposed as follows:



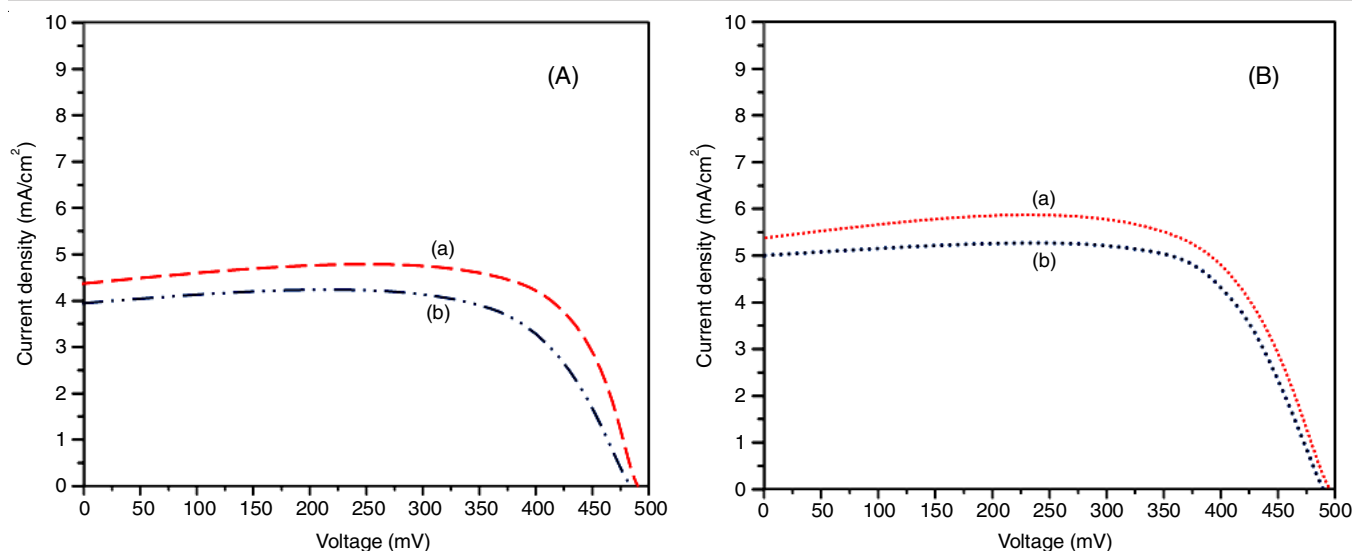


Fig. 8. Current density-voltage (J-V) curves for the DSSCs fabricated from (A) (a) PbO coated GCE in 0.1 M KCl and (b) Cu PbO nanomaterial GCE in 0.1 M KCl by synthetic ruthenium dye (535-bisTBA, N719) and (B) (a) PbO coated GCE in 0.1 M KCl and (b) Cu PbO nanomaterial GCE in 0.1 M KCl by natural fruit extract percent in anthocyanin dye solution

Leuco DG B dye → Products (6)

The diamond green B dye consumes the appropriate wave length and generates an electronically excited state. Intersystem crossing is also used to give a much more durable triplet state. This energy is also used by the CuPbO semiconductor to excite its electron from the valence band to the conduction band. The hole (h^+) located in the valence band of the semiconductor can withdraw an electron from the hydroxyl ion, resulting in the formation of the $\cdot\text{OH}$ radical. The hydroxyl radical will oxidize the diamond green B dye to its leuco form, which could eventually breakdown into products. The presence of hydroxyl radical scavenger (2-propanol) significantly reduced the rate of degradation of diamond green B dye, indicating that the $\cdot\text{OH}$ radical participates as an active oxidizing species in the dye degradation [30-37].

Photovoltaic characteristics (Synthetic based dye sensitized solar cells): CuPbO has the ability to function as a photo-detector. It's deposited on a single crystal made of fluorine doped tin oxide (FTO-plate). A ruthenium dye was used to create two dye-sensitized solar cells made of PbO and CuPbO. (535-bisTBA, N719). From the data, it is obvious that the CuPbO-fabricated cell has a higher short-circuit current density, J_{sc} (4.4 mA/cm^2) than the PbO (3.9 mA/cm^2) fabricated cell. The V_{oc} (500 mV) open-circuit voltage FF (0.94) fill-factor and performance (1.7%) Fig. 8a-b depict the J-V curves. CuPbO improves electron transport in short circuit current density, according to the findings [38,39].

Photovoltaic characteristics (natural-based dye sensitized solar cells): The anthocyanin dye (*Vaccinium myrtillus*) extracted from blueberry fruits was used to manufacture two dye-sensitized solar cells employing PbO and CuPbO. With the maximum value of short-circuit current density, the CuPbO-based cell exhibits better activity as well. The J_{sc} (5.5 mA/cm^2) is higher than PbO (5.0 mA/cm^2) in terms of open-circuit voltage (500 mV), fill-factor (0.94) and efficiency (1.7%).

Conclusion

Subsequently using a simple co-precipitation approach, an effective CuPbO nanomaterial was prepared. The HR-SEM, EDX, HR-TEM and HR-TEM were used to characterize this nanomaterial and UV-vis-DRS studies. The SEM analysis showed that CuPbO has a nanoflower morphology. The high photocatalytic action of CuPbO material be ascribed to the decreased emission intensity and small band gap energy. The nanomaterial CuPbO was found to photodegrade diamond green B dye in deionized water with superior efficiency. The present studies also established that CuPbO can acts as a promising photoelectrode in fabricating dye based (both synthetic and natural) solar cells with enhanced current produced in short circuit.

CONFLICT OF INTEREST

The authors declare that there is no conflict of interests regarding the publication of this article.

REFERENCES

- B. Jia and L. Gao, *Mater. Chem. Phys.*, **100**, 351 (2006); <https://doi.org/10.1016/j.matchemphys.2006.01.012>
- V. Raju, S. Murthy, F. Gao, Q. Lu and S. Komarneni, *J. Mater. Sci.*, **41**, 1475 (2006); <https://doi.org/10.1007/s10853-006-7489-4>
- S. Chen and N. Li, *J. Mater. Chem.*, **12**, 1124 (2002); <https://doi.org/10.1039/b110309a>
- Q. Zhou, X.Y. Liu, L. Liu, Y.G. Li, Z.Y. Jiang and D.Y. Zhao, *Chem. Lett.*, **34**, 1226 (2005); <https://doi.org/10.1246/cl.2005.1226>
- C.L. Juan, Z.S. Mao, W.Z. Shen, Z.Z. Jun and D.H. Xin, *Mater. Lett.*, **59**, 3119 (2005); <https://doi.org/10.1016/j.matlet.2005.05.031>
- X. Jiang, Y. Wang, T. Herricks and Y. Xia, *J. Mater. Chem.*, **14**, 695 (2004); <https://doi.org/10.1039/b313938g>
- K. Nagaveni, G. Sivalingam, M.S. Hegde and G. Madras, *J. Appl. Catal. B*, **48**, 83 (2004); <https://doi.org/10.1016/j.apcatb.2003.09.013>

8. R. Asahi, T. Morikawa, T. Ohwaki, K. Aoki and Y. Taga, *Science*, **293**, 269 (2001);
<https://doi.org/10.1126/science.1061051>
9. H. Ji, W. Ma, Y. Huang, J. Zhao and Z. Wang, *Chin. Sci. Bull.*, **48**, 680 (2003);
<https://doi.org/10.1360/03tb9146>
10. W. Zhao, C. Chen, X. Li, J. Zhao, H. Hidaka and N. Serpone, *J. Phys. Chem. B*, **106**, 5022 (2002);
<https://doi.org/10.1021/jp020205p>
11. H. Ollgaard, L. Frost, J. Gastler and O.C. Hensen, Survey of Azo- Colorants on Denmark: Milgo Danish Environmental Protection Agency, Project No. 509 (1999).
12. A. Stolz, *Appl. Microbiol. Biotechnol.*, **56**, 69 (2001);
<https://doi.org/10.1007/s002530100686>
13. T. Robinson, G. McMullan, R. Marchant and P. Nigam, *Bioresour. Technol.*, **77**, 247 (2001);
[https://doi.org/10.1016/S0960-8524\(00\)00080-8](https://doi.org/10.1016/S0960-8524(00)00080-8)
14. O.D. Uluozlu, A. Sari, M. Tuzen and M. Soylak, *Bioresour. Technol.*, **99**, 2972 (2008);
<https://doi.org/10.1016/j.biortech.2007.06.052>
15. A. Sari, D. Mendil, M. Tuzen and M. Soylak, *Chem. Eng. J.*, **144**, 1 (2008);
<https://doi.org/10.1016/j.cej.2007.12.020>
16. G.R.N. Bidhendi, A. Torabian, H. Ehsani and N. Razmkhah, *J. Environ. Health Sci. Eng.*, **4**, 29 (2007).
17. S. Srivastava, R. Sinha and D. Roy, *Aquat. Toxicol.*, **66**, 319 (2004);
<https://doi.org/10.1016/j.aquatox.2003.09.008>
18. G. Crini, *Bioresour. Technol.*, **97**, 1061 (2006);
<https://doi.org/10.1016/j.biortech.2005.05.001>
19. J. Chen, M. Liu, L. Zhang, J. Zhang and L. Jin, *Water Res.*, **37**, 3815 (2003);
[https://doi.org/10.1016/S0043-1354\(03\)00332-4](https://doi.org/10.1016/S0043-1354(03)00332-4)
20. B. Gao, C. Peng, G. Chen and G. Lipuma, *Appl. Catal. B*, **85**, 17 (2008);
<https://doi.org/10.1016/j.apcatb.2008.06.027>
21. F. Xiu and F. Zhang, *J. Hazard. Mater.*, **172**, 1458 (2009);
<https://doi.org/10.1016/j.jhazmat.2009.08.012>
22. J. Zhang, D. Fu, Y. Xu and C. Liu, *J. Environ. Sci.*, **22**, 1281 (2010);
[https://doi.org/10.1016/S1001-0742\(09\)60251-5](https://doi.org/10.1016/S1001-0742(09)60251-5)
23. S. Sood, S.K. Mehta, A. Umar and S.K. Kansal, *New J. Chem.*, **38**, 3127 (2014);
<https://doi.org/10.1039/C4NJ00179F>
24. B. Subash, B. Krishnakumar, M. Swaminathan and M. Shanthi, *Langmuir*, **29**, 939 (2013);
<https://doi.org/10.1021/la303842c>
25. A. Charanpahari, S.G. Ghugal, S.S. Umare and R. Sasikala, *New J. Chem.*, **39**, 3629 (2015);
<https://doi.org/10.1039/C4NJ01618A>
26. D. Raoufi and T. Raoufi, *Appl. Surf. Sci.*, **255**, 5812 (2009);
<https://doi.org/10.1016/j.apsusc.2009.01.010>
27. H. Hartnagel, A.L. Dawar, A.K. Jain and C. Jagadish, *Semiconducting Transparent Thin Films*, CRC Press (1995).
28. J.I. Pankove, *Optical Progress in Semiconductors*, Dover Publication: New York (1975).
29. S. Rasalingam, H.S. Kibombo, C.M. Wu, R. Peng, J. Baltrusaitis and R.T. Koodali, *Appl. Catal. B*, **148-149**, 394 (2014);
<https://doi.org/10.1016/j.apcatb.2013.11.025>
30. V. Navakoteswara Rao, N. Lakshmana Reddy, M. Mamatha Kumari, P. Ravi, M. Sathish, K.M. Kuruvilla, V. Preethi, K.R. Reddy, N.P. Shetti, T.M. Aminabhavi and M.V. Shankar, *Appl. Catal. B*, **254**, 174 (2019);
<https://doi.org/10.1016/j.apcatb.2019.04.090>
31. D. Li, T. Sun, L. Wang and N. Wang, *Electrochim. Acta*, **282**, 416 (2018);
<https://doi.org/10.1016/j.electacta.2018.06.075>
32. K.R. Reddy, C.H.V. Reddy, M.N. Nadagouda, N.P. Shetti, S. Jaesool and T.M. Aminabhavi, *J. Environ. Manage.*, **238**, 25 (2019);
<https://doi.org/10.1016/j.jenvman.2019.02.075>
33. N.L. Reddy, V.N. Rao, M. Vijayakumar, R. Santhosh, S. Anandan, M. Karthik, M.V. Shankar, K.R. Reddy, N.P. Shetti, M.N. Nadagouda and T.M. Aminabhavi, *Int. J. Hydrogen Energy*, **44**, 10453 (2019);
<https://doi.org/10.1016/j.ijhydene.2019.02.120>
34. E. Haque, Y. Yamauchi, V. Malgras, K.R. Reddy, J.W. Yi, M.S.A. Hossain and J. Kim, *Chem. Asian J.*, **13**, 3561 (2018);
<https://doi.org/10.1002/asia.201800984>
35. P.S. Basavarajappa, B.N.H. Seethya, N. Ganganagappa, R.R. Kakarla and K.B. Eshwaraswamy, *ChemistrySelect*, **3**, 9025 (2018);
<https://doi.org/10.1002/slct.201801198>
36. A. Mishra, A. Mehta, S. Basu, N.P. Shetti, K.R. Reddy and T.M. Aminabhavi, *Carbon*, **149**, 693 (2019);
<https://doi.org/10.1016/j.carbon.2019.04.104>
37. K. Ameta, P. Tak, D. Soni and S.C. Ameta, *Sci. Rev. Chem. Commun.*, **4**, 38 (2014).
38. J. Kamalakkannan, V.L. Chandraboss, S. Prabha, B. Karthikeyan and S. Senthilvelan, *J. Mater. Sci.: Mater. Electron.*, **27**, 2488 (2016);
<https://doi.org/10.1007/s10854-015-4050-8>
39. J. Kamalakkannan, V.L. Chandraboss, B. Loganathan, S. Prabha, B. Karthikeyan and S. Senthilvelan, *Appl. Nanosci.*, **6**, 691 (2016);
<https://doi.org/10.1007/s13204-015-0474-y>